Ring-shaped corona proteins influence the toxicity of engineered nanoparticles to yeast

Environmental Science Nano

PAPER

Ring-shaped corona proteins influence the toxicity of engineered nanoparticles to yeast†

Cite this: DOI: 10.1039/c7en01226h

Roberta Ruotolo,[a] Graziella Pira,[a] Marco Villani,[b] Andrea Zappettini[b] and Nelson Marmiroli *[ac]

Engineered nanoparticles (ENPs) have found applications in different fields varying from medical science to electronics. The increasing interest in these materials, fuelled by the potential benefits of their use, has not as yet been matched by a concerted effort to gain a full understanding of potential negative effects they may have on the environment and on human health. In a biological environment, ENPs become coated by a so-called "protein corona", the structure of which defines their biological identity. The present research set out to characterize the interaction between cadmium sulphide quantum dots (QDs) and yeast cells, isolating and identifying the set of proteins which were adsorbed on the QD surface using liquid chromatography-mass spectrometry followed by an *in silico* protein analysis. Ring-shaped proteins were particularly prone to binding, and electrostatic and hydrophobic interactions were central for this interaction. QDs strongly increased the transcript levels of genes encoding the major hard corona proteins indicating a mechanism of genetic compensation in response to the "physical sequestration" of these proteins in the QD corona *in vivo*. The toxicological implications of the protein corona formation were explored using yeast mutant strains carrying deletions in genes encoding the corona proteins. Interestingly, these mutants were tolerant to doses of QDs that were lethal to wild type cells. These results reveal that the hard protein corona mediates the toxicity of QDs in yeast and a major resolution of this interaction at the molecular level is crucial for a better understanding of the *in vivo* response of ENPs.

Received 19th December 2017,
Accepted 29th April 2018

DOI: 10.1039/c7en01226h

rsc.li/es-nano

Environmental significance

The formation of protein corona has a central role in biological identity and environmental fate of engineered nanoparticles (ENPs), but understanding of ENP–corona interactions and their molecular implications are largely absent from the literature. In this study the use of yeast *S. cerevisiae* as a model has shown how hard corona formation can be linked to CdS QD toxicity. We identify several proteins able to fold in ring-shaped structures that form the hard corona and were crucial in defining the bioactivity of these ENPs. Understanding the effects of these bio-nano interactions at molecular and physiological level can have a direct impact on the safe and sustainable development and use of ENPs in biotechnology and nanomedicine.

Introduction

Rapid advances in nanotechnology over recent years have promoted a range of applications in various fields.[1] The unique properties of engineered nanoparticles (ENPs) have attracted particular interest.[2] Yet, their potential for harm remains clouded by a lack of understanding of how they interact with living matter.[3,4] In a biological environment, ENPs are known to selectively adsorb proteins, along with certain other compounds, to form a 'corona' bound tightly to their surface.[5–9] The nature of the corona is a major determinant of ENP toxicity and so is an important issue in considering the deployment of ENPs in biological systems.[5–14] The strength of the protein–ENP interaction is known to be influenced by the size and surface properties of the ENPs,[10] while the formation of the corona involves an element of

[a] *Department of Chemistry, Life Sciences and Environmental Sustainability, University of Parma, Parma, Italy. E-mail: nelson.marmiroli@unipr.it; Fax: +39 0521 906222; Tel: +39 0521 905606*
[b] *Institute of Materials for Electronics and Magnetism (IMEM), National Research Council (CNR), Parma, Italy*
[c] *The Italian National Interuniversity Consortium for Environmental Sciences (CINSA), Parma, Italy*

† Electronic supplementary information (ESI) available: Supplementary figures show some physico-chemical analysis performed for the characterization of CdS QDs (Fig. S1), the proteomic analysis of the yeast proteins adsorbed onto the surface of CdS QDs (Fig. S2), the documented interactions (physical and genetic) between the hard corona proteins (Fig. S3) and the AFM analysis of the CdS QD-protein corona (Fig. S4). Supplementary tables report the average hydrodynamic diameter of CdS QDs in water and yeast culture medium (Table S1), the list of primers used in real-time PCR analysis (Table S2), the amino acid frequencies in the corona protein polypeptides (Table S3), and the yeast protein structures available in the PDB database (Table S4). Additional experimental details were also included in ESI. See DOI: 10.1039/c7en01226h

competition between several proteins in a dynamic process which involves their adsorption/desorption on the ENP surface.[15,16] Corona proteins which show a high affinity for the ENP surface are exchanged slowly, and these so-called "hard" proteins form the innermost layer, while the "soft" proteins are more loosely bound, possibly through protein–protein interactions, and are rapidly exchanged.[8,16,17]

Quantum dots (QDs), a class of ENPs based on a semiconductor crystal of nanometre dimensions, have featured in both fundamental research and industrial development.[18–21] Both *in vitro* and *in vivo* studies with a range of QDs have shown that toxicity is closely related to QD surface properties, diameter and ligand stability in biological media.[20,22]

Nevertheless, few reports on the QD–cell interaction at the molecular level in *Saccharomyces cerevisiae* have been published,[23–26] and, to our knowledge, no paper was focused on the QD formation in yeast. Exposure to CdS QDs has been shown to increase the synthesis of reactive oxygen species (ROS), disrupt mitochondrial membrane potential and affect mitochondrial morphology in yeast,[26] but the mechanistic basis for these effects are not as yet fully understood.

The budding yeast *S. cerevisiae* is a powerful model organism for studying fundamental aspects of eukaryotic cell biology.[27] The availability of an advanced selection of genetic tools available for this organism (*e.g.*, yeast genome-wide collections of mutant strains) and its well-known physiology have indeed facilitated target identification of several bioactive compounds.[27,28] *In vivo* chemical inhibition of a gene product (protein) is expected to yield similar results as a loss-of-function mutation, and genomic phenotyping studies can be integrated with chemical-induced gene expression profiling to link a compound to its cellular target.[27]

For these reasons, the aim of this research was to investigate the formation of the hard protein corona on the CdS QD surface and to study whether the identity of these proteins has an influence over their bioactivity in *S. cerevisiae*. The paper describes the identification and functional characterization of the hard corona proteins adsorbed on the surface of CdS QDs in yeast cells. Given the relationship between the adsorption of an enzyme onto an ENP and the inhibition of its activity (see ref. 29–35 for some relevant examples taking into account this issue) the identification of which proteins are components of the QD corona can in fact elucidate the biochemical nature of their toxicological response.

Experimental

Synthesis and characterization of the CdS QDs

The synthesis and characterization of water-soluble CdS QDs has been described elsewhere,[25,26,36] and some additional experimental details were reported in "ESI†". Briefly, X-ray diffraction (XRD) and transmission electron microscopy (TEM) analysis showed that CdS QDs exhibited hexagonal shape and a mean diameter of 5 nm (Fig. S1A and B†).

Prior to their use, the CdS QDs were exposed for 16 min to sonication in a Transsonic 460 bath (Elma Electronic AG) to reduce ENP agglomeration. Z-potential and particle size distribution by dynamic light scattering (DLS) analysis were performed using a NanoBrook ZetaPALS analyzer (Brookhaven Instruments). Table S1† reported the average hydrodynamic diameters of CdS QDs in water and yeast culture medium incubated at 28 °C for 24 h with gently shaking. The hydrodynamic diameter of CdS QDs in these experimental conditions was comparable (Table S1†).

Atomic absorption spectroscopy (AAS) analysis of the Cd^{2+} ion concentration in different experimental samples (Fig. S1C†) was performed using the 240FS AA spectrometer (Agilent Technologies) as previously described.[37]

Yeast strains and culture

The yeast wild type strain BY4742 (*MATα his3Δ1 leu2Δ0 lys2Δ0 ura3Δ0*) and five haploid deletion strains (*tdh2Δ*, *tdh3Δ*, *pdc1Δ*, *eft2Δ*, *hsc82Δ*) available in the Yeast Knockout Collection (GE Dharmacon) were used. The set of TAP-tagged strains (BY4741 background strain: *MATa his3Δ1 leu2Δ0 met15Δ0 ura3Δ0*) were selected from the yeast TAP-tagged ORF library (GE Dharmacon). Cells were grown at 30 °C on either yeast extract peptone (YPD) or on a synthetic medium (SD) supplemented with 2% (w/v) glucose.

Protein extraction

Pelleted yeast cells (1E8 cells) were rinsed in ice cold phosphate-buffered saline (PBS) and re-suspended in cold 200 mM Tris-HCl (pH 8.0), 150 mM ammonium sulphate, 10% (v/v) glycerol, containing protease inhibitor cocktail (Sigma Aldrich). Acid-washed glass beads were added in order to mechanically lyse the cells using a Thermo Savant FastPrep® Cell Disrupter (Qbiogene Inc.). After vortexing (four times @ 45 s, twice @ 10 s, with a 5 min rest on ice between vortexings), the lysate was clarified by centrifugation (30 min, 21 000*g*, 4 °C). The concentration of protein in the lysate was determined using both a Bradford assay (BioRad) and Pierce™ BCA protein assay kit (Thermo Fisher Scientific).

Assay for binding to CdS QDs

The yeast cell lysate (7 g L^{-1} protein) was incubated in the presence of 0.5 g L^{-1} CdS QDs in 200 mM Tris-HCl (pH 8.0), 150 mM ammonium sulphate, 10% (v/v) glycerol at 4 °C for 24 h with gentle agitation, following Sund *et al.*[38] The QDs, along with their adsorbed corona proteins, were recovered by centrifugation (21 000*g*, 5 min, 4 °C), and unbound proteins were removed by rinsing the pellet five times in salt-free buffer [20 mM Tris-HCl (pH 7.4)], followed by three times in salt-buffered solution [0.1 M NaCl, 20 mM Tris-HCl (pH 7.4)]. After each rinse, the pellets were gently vortexed and re-centrifuged (21 000*g*, 5 min, 4 °C). Hard corona proteins were stripped from the QDs by a 1 h incubation at 30 °C in resuspension buffer [60 mM Tris-HCl (pH 6.8), 2% (w/v) SDS, 10% (v/v) glycerol], then held at 100 °C for 5 min.

For visualization, the proteins were denatured by holding at 95 °C for 5 min in 62.5 mM Tris-HCl (pH 6.8), 2.5% (w/v) SDS,

0.02% (w/v) bromophenol blue, 2% (v/v) β-mercaptoethanol, 10% (v/v) glycerol, then separated electrophoretically through 12% (w/v) SDS polyacrylamide gels.

In experiments designed to evaluate electrostatic interactions between ENPs and corona proteins, proteins were eluted from the QDs by a 1 h incubation at 30 °C with gentle agitation in different buffered solutions, as indicated: 20 mM sodium acetate, pH 5 (acidic pH); 20 mM Tris-HCl, pH 8.5 (basic pH); denaturing buffer [4% (w/v) SDS, 572 mM β-mercaptoethanol, PBS)]. The concentration of released corona proteins was determined using the Pierce™ BCA protein assay kit.

For AFM analysis, CdS QD–corona protein pellet was resuspended in PBS buffer (2 ml). A drop of CdS QD–protein suspension (20 μl) was deposed onto freshly cleaved mica and incubated for 5 minutes at room temperature; the disk was then rinsed with MilliQ water and dried with a gentle nitrogen flow. AFM imaging was performed on the dried sample with a Nanoscope IIIa microscope equipped with scanner J and operating in tapping mode. Commercial diving board silicon cantilevers (MikroMasch, Tallinn, Estonia) were used.

Protein digestion and LC-MS/MS analysis

Re-suspended corona proteins were denatured by the addition of 6 M urea in 25 mM ammonium bicarbonate. Disulphide bonds were reduced by adding DTT to a final concentration of 35 mM and holding for 1 h at room temperature, and reduced cysteine residues were alkylated by adding iodoacetamide to a final concentration of 32 mM and holding for 1 h at room temperature in the dark. After the urea concentration had been lowered to 0.6 M by dilution with 25 mM ammonium bicarbonate, trypsin (Sigma Aldrich) was added in a 1 : 30 (w/w) ratio, and the digestion allowed to run for 18 h at 37 °C. The reactions were stopped by adding formic acid to a final concentration of 0.5% (w/v) and incubating with gentle agitation at 37 °C for 15 min; thereafter the solutions were lyophilized using a Speedvac device (Savant). The dried samples were re-suspended in 0.1% (w/v) formic acid and subjected to liquid chromatography-mass spectrometry (LC-MS/MS), using a Dionex Ultimate 3000 micro HPLC device coupled to an LTQ-Orbitrap XL mass spectrometer equipped with a conventional electrospray ionization source (Thermo Fisher Scientific).[39] Information regarding known yeast protein sequences was retrieved from the UniProt database (www.uniprot.org). The experiments were carried out as two biological replicates and three technical replicates. Proteins were considered part of the hard corona of the CdS QDs if identified in at least five replicates. *Coverage* (%) represents the ratio between the number of residues in all found peptides and the total number of amino acids in the entire protein sequence. *Score* was based on the probability (*P*) that the observed match between the experimental data and the database sequence was not a random event.[39] Protein identifications (Table 1) were accepted with a coverage greater than 35% and a score of at least 70%. We used a false recovery rate minor of 1% as the cutoff criterion for peptide and protein identification.

Real-time PCR

Yeast cells were grown either in the presence or absence of 250 mg L^{-1} CdS QDs in YPD medium at 30 °C for 2 h. Cells (2E6 cells) were pelleted by centrifugation and total RNA was extracted from the pellet using an RNeasy® kit (Qiagen) following the manufacturer's protocol. A 1 μg aliquot of the resulting RNA was converted to cDNA using a Quantitect Reverse Transcription kit (Qiagen), as described by the manufacturer. The primers used in subsequent real-time PCRs were designed using Primer Express® software (Applied Biosystems): their sequences are given in Table S2.† Real-time PCR was performed with a ABI PRISM 7000 Sequence Detection System (Applied Biosystems) and *Power* SYBR® Green RT-PCR Mix (Thermo Fisher Scientific) according to the manufacturer's instructions. *ACT1* was used as the reference sequence. Each of the primer pairs amplified only a single product (of size 67–114 bp) when conventional reverse transcription-PCR amplicons were separated by agarose gel electrophoresis. Melting curve analyses were conducted to check for amplification specificity. Each reaction was

Table 1 Yeast hard corona proteins identified by LC-MS/MS analysis

Corona protein	Description (UniProt accession N.)	Coverage[a] (%)	Score[b]	pI	Molecular weight (kDa)	Biological process
Cdc19	Pyruvate kinase (P00549)	46.8	85.9	7.6	54	Energy metabolism
Pdc1	Pyruvate decarboxylase isozyme 1 (P06169)	71.2	308.7	5.8	61	
Tdh2	Glyceraldehyde-3-phosphate dehydrogenase (P00358)	74.7	186.8	6.5	36	
Tdh3	Glyceraldehyde-3-phosphate dehydrogenase (P00359)	83.7	181.6	6.5	36	
EF-1α (Tef1/2)	Translation elongation factor 1-alpha (P02994)	75.8	285.9	9.1	50	Translation process
eEF-2 (Eft1/2)	Elongation factor 2 (P32324)	36.3	72.15	5.9	93	
Yef3/EF-3A	Translation elongation factor 3 (P16521)	56.9	313.7	5.7	116	
Hsc82	Cytoplasmic chaperone of the Hsp90 family (P15108)	46.8	144.2	4.5	81	Molecular chaperoning
Ssb2	Ribosome-associated molecular chaperone (P40150)	48.6	73.9	5.4	66	

[a] Coverage (%) represents the ratio between the number of residues in all found peptides and the total number of amino acids in the entire protein sequence. [b] Score was based on the probability (*P*) that the observed match between the experimental data and the database sequence was not a random event.[39]

conducted in triplicate, and included a no template control. Relative transcript abundances were derived using the $2^{-\Delta\Delta CT}$ method.[40]

Western blotting

Yeast TAP-tagged strains (Yef3-TAP-tag, Eft2-TAP-tag, SSb2-TAP-tag, Tdh2-TAP-tag, Tdh3-TAP-tag, Pdc1-TAP-tag) were grown either in the presence or absence of 250 mg L^{-1} CdS QDs in YPD medium at 30 °C for 6 h, after which the cells were harvested and lysed as described above. Total protein extracts (10 μg per sample) were electrophoretically separated through 12% SDS polyacrylamide gels and transferred to a nitrocellulose membrane (Thermo Fisher Scientific). The membranes were blocked by bathing in Tris-buffered saline containing 0.1% (v/v) Tween20 and 5% (w/v) skimmed milk (TTS buffer). The membranes were initially challenged with rabbit anti-TAP-tag polyclonal antibody (CAB1001, Open Biosystems; 1 : 2000 dilution) in TTS buffer overnight at 4 °C, and reacting proteins were visualized using the Odyssey® Imaging System (LI-COR) following hybridization with IRDye 680RD labeled goat anti-rabbit antibody (1 : 10 000 dilution). Mouse anti-Pgk1 monoclonal antibody (Abcam; 1 : 5000 dilution) was used as a control.

Spot assay

The wild type strain BY4742 and the set of haploid mutant strains were grown at 30 °C in YPD medium. After 24 h, optical densities at 600 nm (OD_{600}) were determined using a Cary 50 UV-visible spectrophotometer (Varian), and the OD_{600} was adjusted to 1.0 with sterile water; the cells were then serially diluted in tenfold decrements.[41] Aliquots (4 μL) of each dilution were spotted onto SD-agar plates in the presence or absence of CdS QDs (20–250 mg L^{-1}). The growth of the cells was monitored after incubation at 30 °C for two days.

GAPDH activity assay

A GAPDH Activity Assay Kit supplied by Abcam was used to quantify GAPDH, following the manufacturer's instructions. A 1 μg aliquot of yeast protein extract, along with 0.1–20 mg L^{-1} CdS QDs, were added to the kit reagents and the reaction allowed to run for 60 min at 37 °C. The absorbance of the reaction was read at 450 nm using the iMark™ Microplate Absorbance Reader (Bio-Rad).

Polypeptide sequence analysis

A global set of yeast polypeptide sequences was obtained from the Saccharomyces Genome Database (www.yeastgenome.org/), from which a global mean amino acid frequency was determined. The amino acid frequency for specific proteins was used to compute a protein-specific amino acid Z-score, given by the expression (protein-specific amino acid frequency − average amino acid frequency)/global standard deviation. The Z-score reflects whether a given residue is over- or under-represented. Corresponding *P*-values were determined for all over-represented or under-represented residues, using a one-tailed *t*-test. RasMol (http://www.openrasmol.org/), CASTp[42] and PDPsum (www.ebi.ac.uk/pdbsum/) softwares were used to analyze protein structure.

Statistical analysis

Each experiment was represented by three to five technical replicates and two biological replicates. All statistical analyses were performed using routines implemented in GraphPad Prism v6 software.

Results and discussion

Identification of proteins with high affinity for CdS QDs

To identify yeast proteins adsorbed on the ENP surface, CdS QDs and protein extracts were incubated with gentle agitation in a medium that replicate the features of the *in vivo* biological milieu. After incubation for different times of exposure (1–24 h) and temperature of incubation (4–37 °C), the ENPs and corona proteins were recovered by centrifugation and the unbound proteins washed out followed by resuspension in wash buffer. The adsorbed proteins were recovered from the ENP surface and analyzed with SDS-polyacrylamide gel electrophoresis (SDS-PAGE) to estimate molecular masses and relative abundance (Fig. S2;† see "Experimental" for additional details). Visual evaluation of the SDS-PAGE separations showed that the quantity of protein adsorbed responded both to the concentration of protein in the incubation solution (Fig. S2A†) and to the time allowed for incubation (Fig. S2B†). There was no significant qualitative difference between the protein profiles. Binding assays performed at 4 °C and 37 °C generated neither qualitative nor quantitative differences (Fig. S2C†). The optimal incubation conditions for binding were to expose Cd QDs to yeast proteins for 24 h at 4 °C, to minimize protein degradation.

Multiple centrifugation steps and extensive washes with buffers of different ionic strengths were used to release almost all nonbound and soft corona proteins. Hard corona proteins were eluted out from the ENP surface and identified (after tryptic digestion) using liquid chromatography-high-resolution mass spectrometry (LC-MS/MS; see "Experimental" for additional details). The hard corona was found to be composed of a number of distinct proteins varying in molecular weight between 30 and 100 kDa (Table 1 and Fig. 1A). The predominant ones were involved either in energy metabolism, in translation or were members of a molecular chaperone superfamily (Table 1). The first group comprised Cdc19 (pyruvate kinase), Pdc1 (pyruvate decarboxylase) and Tdh2 and Tdh3 [two isoforms of glyceraldehyde-3-phosphate dehydrogenase (GAPDH)]. The homotetrameric Cdc19 protein acts during glycolysis to convert phosphoenolpyruvate to pyruvate, and represents a key controller of carbon flux.[43,44] Pdc1 is the most ubiquitous form of the three yeast pyruvate decarboxylases and is involved both in the anaerobic fermentation of pyruvate to acetaldehyde and carbon dioxide, and in amino acid catabolism.[45,46] GAPDH is a glycolytic enzyme which

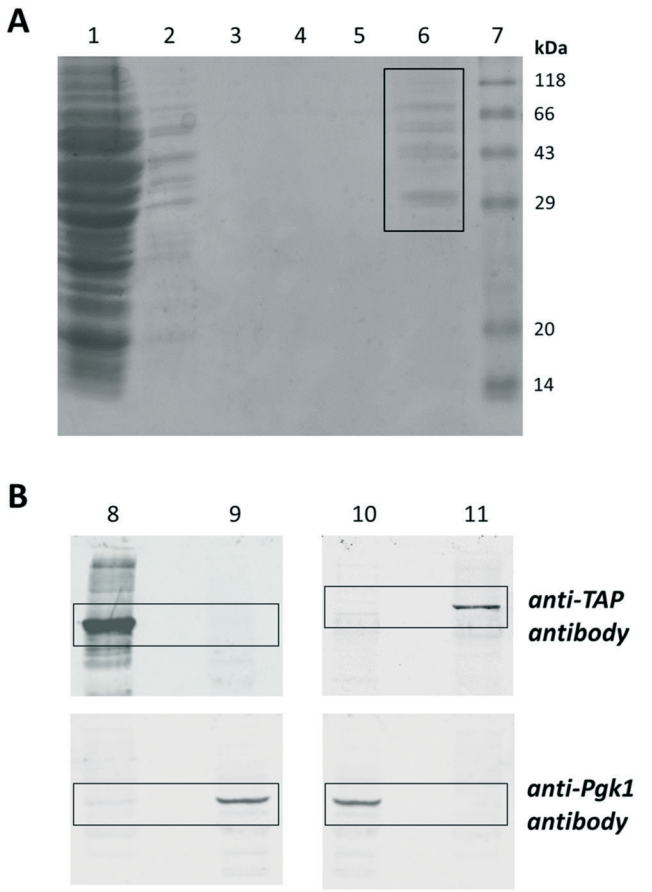

Fig. 1 A set of yeast proteins were associated with the hard corona deposited on the surface of CdS QDs. (A) Aliquots of the wash solutions (lanes 1–5; 30% of the total sample) and yeast-derived hard corona proteins (lane 6; 15% of the total sample) show that the hard corona was composed of proteins varying in molecular weight between 30 and 100 kDa. Lanes 1–3: the first, third and fifth salt-free washes of the CdS QD–protein pellet; lanes 4 and 5: the first and third washes using a salt-buffered solution (see "Experimental" for additional details). Lane 7: molecular weight ladder. (B) Western blot analysis. CdS QDs were incubated with yeast protein extracts obtained from Tdh2-TAP-tag (lane 8) and Pdc1-TAP-tag (lane 11) strains and corona proteins were recovered from QDs by a centrifugation-washing procedure. The adsorbed proteins were eluted out from the ENP surface and analyzed by western blot using an anti-TAP antibody (upper panel); an anti-Pgk1 monoclonal antibody served as a negative control (lower panel). Results obtained showed the presence of these corona proteins in the fractions adsorbed to the CdS QD surface (lanes 8 and 10). Levels of Pgk1, an abundant protein not present in CdS QD–corona, were detected only in yeast extracts obtained from wild type strain (lanes 9 and 10).

catalyses the conversion of glyceraldehyde-3-phosphate to 1,3 bis-phosphoglycerate, but also displays non-glycolytic activity in certain subcellular locations.[47,48]

Three of the hard corona proteins were involved in polypeptide chain elongation (Table 1), namely EF-1α (translation elongation factor 1α, encoded by the genes *TEF1* and *TEF2*), eEF-2 (elongation factor 2, encoded by *EFT1* and *EFT2*), Yef3/EF-3A (elongation factor 3A). EF-1α binds to and delivers aminoacylated tRNA to the ribosomal A-site during protein synthesis,[49] and is also thought to target damaged proteins to the proteasome.[50] eEF-2 catalyses GTP-dependent ribosomal translocation during translation elongation.[51] Yef3/EF-3A is required for the ATP-dependent release of deacylated tRNA from the ribosomal E-site during protein synthesis and also stimulates the EF-1α-dependent binding of aminoacyl-tRNA to the ribosomal A-site.[52]

The other predominant hard corona proteins were two polypeptides involved in molecular chaperoning (Table 1). Ssb2 is a ribosome-associated member of the HSP70 family which participates in the folding of newly-synthesized polypeptides.[53] Hsc82, a member of the HSP90 family,[54] acts to promote the maturation, structural maintenance and regulation of proteins involved in cell cycle control, ribosome stability and signal transduction.[54,55] Notably, Hsp90 proteins are also known to operate in a number of the signaling pathways which are altered as a result of ENP exposure.[56,57] Ssb2 and Hsp82 share many common protein interactors, suggesting functional collaboration among these chaperones.[58]

Yeast strains in which Pdc1 and Tdh2 were TAP-tagged were used to confirm that these two proteins were a component of the hard corona (Fig. 1B). CdS QDs were incubated with protein extracts obtained from Pdc1-TAP-tag and Tdh2-TAP-tag strains and CdS QD–corona proteins were recovered by a centrifugation-washing procedure. The adsorbed proteins were eluted out from the ENP surface and analyzed by western blot using an anti-TAP antibody (Fig. 1B); anti-Pgk1 monoclonal antibody served as a negative control. Results obtained showed the presence of these corona proteins in the fractions adsorbed to the CdS QD surface (Fig. 1B). Levels of Pgk1, an abundant protein not present in CdS QD–corona, were detected only in yeast extracts obtained from wild type strain.

CdS QDs affect the transcript levels and the abundance of corona proteins

In vivo formation of protein corona on CdS QD surface could affect the expression of the corona proteins themselves. Therefore, we have conducted experiments to evaluate if the genes encoding the major corona proteins were modulated at transcriptional level by CdS QDs. Yeast wild type strain (BY4742) was grown for 2 hours with or without CdS QD treatment (250 mg L^{-1}), total RNA was extracted and cDNAs were synthesized. Real-time PCR was performed on cDNA prepared from treated and untreated samples, using *ACT1* as housekeeping gene. Gene expression analysis showed that all of the genes encoding the major hard corona proteins were up-regulated by CdS QD treatment (Fig. 2A). *CDC19*, the most strongly up-regulated gene (Fig. 2A), encodes a glycolytic enzyme, which is essential during fermentation.[43] The modulation of this gene by the presence of CdS QDs suggests that energy metabolism is impaired by the ENP-induced stress, an effect which has also been shown in an earlier study.[26] The strong up-regulation of *SSB2* (Fig. 2A) may be necessary to maintain the correct folding of the newly translated proteins

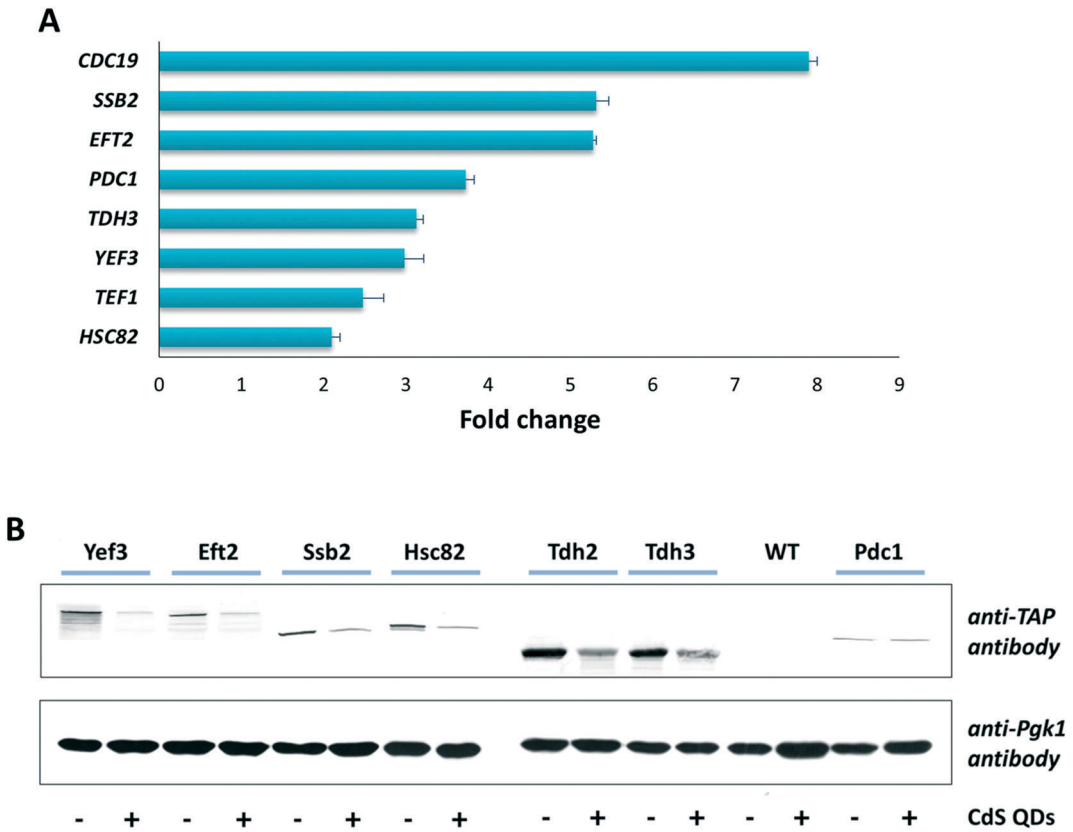

Fig. 2 CdS QDs affect the mRNA expression and the abundance of corona proteins. (A) Genes encoding the major corona proteins were up-regulated in response to the CdS QD treatment; transcript abundances were normalized to that of the reference sequence *ACT1*. Histograms in the graph represent mean values of two independent reactions performed in triplicate. (B) CdS QD treatment reduced the abundance of a set of corona proteins. Protein extracts obtained from TAP-tagged strains and wild type cells (WT) grown either in the presence (+) or the absence (–) of CdS QDs were analyzed by western blot. Protein extract from WT was used as a negative control. Upper panel: the levels of the corona proteins Yef3, Eft2 (eEF-2), Ssb2, Tdh2, Tdh3 and Pdc1 were detected by probing with an anti-TAP antibody. Lower panel: the abundance of Pgk1 was unaffected by the treatment, so served as a loading control.

and to prevent an ENP-induced deleterious protein aggregation and/or misfolding.[35,57,59–61]

It was also evaluated how CdS QD exposure affects the abundance of the proteins identified in ENP corona (Fig. 2B). Wild type and strains from the yeast TAP-tagged ORF library (Yef3-, Eft2-, Ssb2-, Hsc82-, Tdh2-, Tdh3- and Pdc1-TAP-tag) were grown for 6 h with or without CdS QD treatment. Total protein extracts were subjected to western blot analysis (see "Experimental" for details). The protein levels of Cdc19 and EF-1α were not analyzed in this work because their TAP-tagged strains are not present in the yeast library. As shown in Fig. 2B, CdS QDs reduced the abundance of six out of seven of the corona proteins. In particular, the levels of two elongation translational factors (Yef3/EF-3A and Eft2/eEF-2) were strongly reduced by QD treatment (Fig. 2B). The adsorption of these proteins on the QD surface could result in their functional inactivation and consequently reduce the translational levels of other proteins, as is the case for silica ENPs.[62] As confirmation, Pdc1, the levels of which were unaffected by the QD treatment (Fig. 2B), exhibited no evidence of physical interaction with the translational factors identified as present in the hard corona (Fig. S3†).

Protein adsorption is related to ENP toxicity

To assess the roles played by yeast corona proteins in modulating cell viability after exposure to CdS QDs, a phenotypic screening was conducted by examining the fitness of yeast mutant strains carrying deletions in genes encoding the major corona proteins (Fig. 3). The growth of the yeast deletion strains *hsc82Δ*, *tdh2Δ*, *tdh3Δ*, *pdc1Δ* and *eft2Δ* when challenged by a range of concentrations (20–250 mg L^{-1}) of CdS QDs was subsequently examined. Yeast strains deleted in *CDC19*, *YEF3*, *SSB2* and *TEF1/2* genes are not present in yeast haploid deletion mutant collection and are not tested in our analysis. Serial dilution assays of wild type cells and haploid mutant strains were performed on standard synthetic media supplemented with glucose (2%) as carbon source (SD) in the absence or in the presence of CdS QDs (Fig. 3). Minimal growth medium was chosen for these assays to evaluate the toxicological effects of these ENPs in the absence of additional media proteins capable of influencing the protein corona formation. The mutant strains showed a tolerant phenotype also in the presence of high concentrations of CdS QDs (250 mg L^{-1}) that suppress the viability of the wild type strain

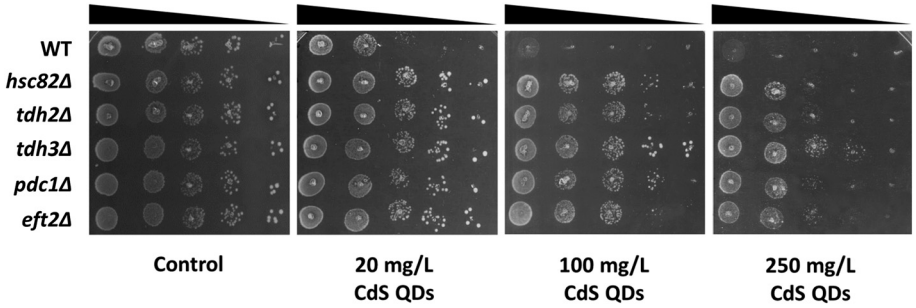

Fig. 3 Mutations in genes encoding hard corona proteins affect cell viability. A spot assay was conducted to compare the growth of wild type (WT) and a range of haploid mutant strains exposed to an increasing concentration of CdS QDs (20–250 mg L^{-1}).

(Fig. 3). Interestingly, none of these mutants exhibited sensitivity or tolerance to Cd^{2+} ion treatment[63] indicating that CdS QD dissolution and release of metal ions in yeast media (not highlighted in our experimental conditions; Fig. S1C†) was not the cause for their resistance to these ENPs. Therefore, CdS QD-tolerant phenotype of these mutant strains suggests that the formation of the protein corona may be crucial in the *in vivo* response to QDs in yeast. ENPs may induce an aberrant conformation of the epitopes of these proteins,[6,64] that may aggregate or promote the binding of the ENPs with other cellular components; this "second type" of interaction could trigger inappropriate cellular processes.[61,65]

In addition, several studies had shown that proteins adsorbed onto ENP surface may result in unfolding with consequent loss of their functionality.[33,35,66] Since two of the three GAPDH isoforms have been found among the corona of these ENPs (Table 1), an *in vitro* enzymatic activity assay (see "Experimental" for details) was used to query whether the protein adsorption on CdS QD surface reduced GAPDH activity. A CdS QD dose-dependent inhibition of the overall activity of yeast GAPDH was observed (Fig. 4). A QD dose-dependent inhibition of GAPDH activity was similarly noted for isoforms of this enzyme in both rabbit and mouse.[34] The active site of GAPDH is surrounded by positively charged residues, the structure of which can be altered by its interaction with the QDs, thereby reducing the accessibility of negatively charged substrates such as GAP.[34] A critical cysteine residue at the active site[67] is present in yeast, rabbit, mouse and human versions of this enzyme, so it is possible that the same binding mechanism works in yeast as operates in the other species.

Notably, the *tdh3Δ* mutant exhibited a higher tolerance (not a sensitivity) than wild type when exposed to concentrations of CdS QDs (20 mg L^{-1}; Fig. 3), which strongly reduced the GAPDH activity *in vitro* (Fig. 4). These results suggest that additional functions of Tdh3 may explain the contribution of the corona to the toxic effect of CdS QDs on yeast cells. Tdh3 is the major GAPDH isoenzyme in *S. cerevisiae*,[68,69] but is also implicated in a variety of cellular processes beyond metabolism, including RNA binding, DNA replication and the maintenance of genomic integrity.[47,48] Tdh3, and to a lesser extent Tdh2, unlike Tdh1 (a GAPDH isoform not identified in the CdS QD corona), promotes Sir2-dependent gene silencing independently of its role in glycolysis by maintaining a sufficient level of NAD^+ to allow Sir2 to function.[48]

In silico analysis of yeast corona proteins

A comparison of the pI (Table 1), amino acid composition and structural features of the corona proteins is shown in Tables S3 and S4.† The majority had a pI < 6.5, implying their carrying a net negative charge at physiological pHs, and suggesting that their adsorption may be mediated by electrostatic interactions. Zeta potential measurements (−17.45 ± 1.14 mV) at physiological pH indicated that the CdS QD suspension was moderately stable and that the CdS QDs had a low negative charge under the experimental conditions used. In experiments designed to evaluate whether electrostatic interactions were established between the hard corona and the CdS QDs, the proteins were eluted from CdS QDs without denaturation using different buffered solutions (Fig. 5A). At a pH of 5, the net charge of most of the corona proteins was positive and they were tightly bound to the CdS QDs (Fig. 5A).

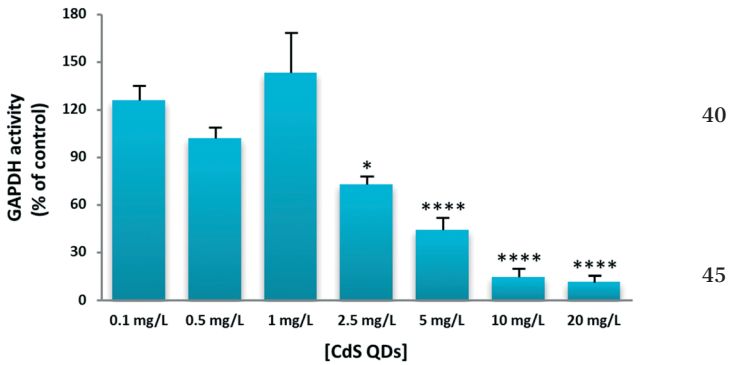

Fig. 4 Inhibition of GAPDH activity by CdS QDs. GAPDH Activity Assay Kit (Abcam) was used following the manufacturer's instructions (see "Experimental" for additional details). The effect of adding a range (0.1–20 mg L^{-1}) of CdS QDs to the reaction mix was assessed. A control reaction (100%) with the reaction mix without CdS QDs was also tested. Data are reported as means ± SD. The statistical significance of differences between means was determined following an analysis of variance; the Bonferroni multiple comparisons test was applied and the threshold for significance was set to 0.05 (*, *P*-value ≤0.05; ****, *P*-value ≤0.0001).

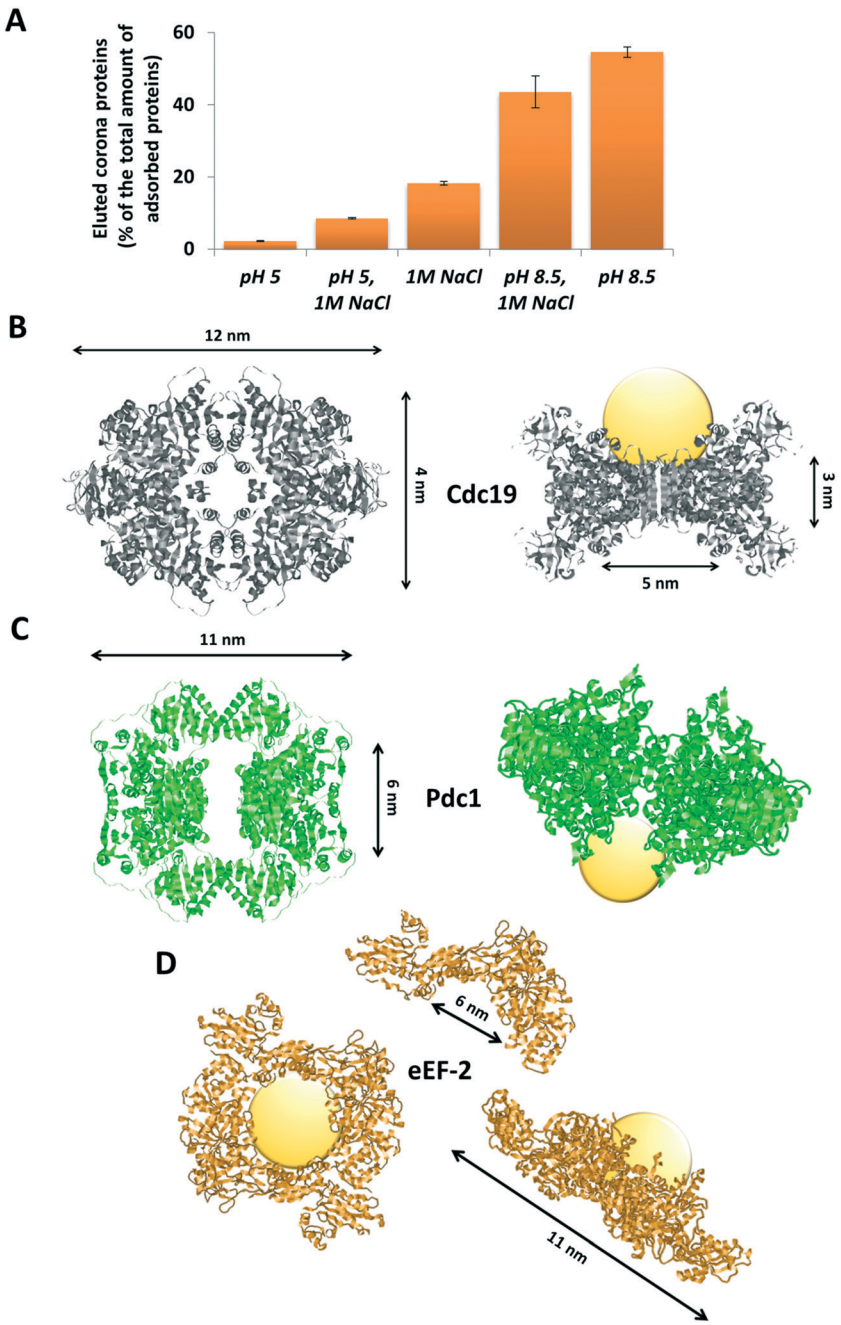

Fig. 5 The structure of selected corona proteins. (A) Electrostatic interactions are at least partially responsible for the formation of the ENP corona. QD–corona proteins were incubated for 1 h with gentle agitation in different buffered solutions and the concentration of released proteins was determined using the PierceTM BCA protein assay kit. At an acidic pH (20 mM sodium acetate, pH 5), the net charge of most of the corona proteins is positive (Table 1) and the yeast proteins remain tightly bound to the CdS QDs; at a basic pH (20 mM Tris-HCl, pH 8.5), the net charge of most of the corona proteins is negative (Table 1) and electrostatic repulsion between the QDs and the proteins favors the protein release from the ENP surface. Added salt (1 M NaCl) reduces the protein adsorption at pH 5. The total amount of adsorbed proteins on the QD surface (100%) was determined by heating at 100 °C for 5 minutes in denaturing buffer (see "Experimental" for additional details). (B–D) Three dimensional models of the putative CdS QD-binding sites. Top and lateral views of (B) Cdc19, (C) Pdc1, (D) eEF-2 adsorbed onto CdS QDs (yellow spheres) display either ring (B and C) or semi-ring (D) structures. Protein structure images are produced using RasMol software.

At pH 8.5, most of the corona proteins became negatively charged and about half of the bound protein was successfully eluted from the QDs (Fig. 5A). These observations implied that the adsorption was at least partially mediated by electrostatic forces, involving positively charged regions on the protein surface. The effect of adding NaCl to the elution buffer was to significantly decrease the level of adsorption at pH 5, but not at pH 8.5 (Fig. 5A), observations which were taken to suggest that clusters of polar and/or basic residues were partially involved in the binding process.

Electrostatic interactions are known to be important during the adsorption of proteins onto a hydrophilic surface.[6,70–72] Z-potential measures indicated that the CdS QDs were negatively charged, so it was unexpected to find that most of the hard corona proteins identified here carried net negative charge at the physiological pH, as is also the case for other proteins which are adsorbed onto QDs: for example, GroEL (pI of 4.7), BSA (pI of 4.7), bacteriophage P22 coat protein (pI of 4.97) and human haemoglobin (pI of 6.9).[32,73–76] It has long been recognized that the binding strength of a protein can be determined by a small number of charged groups located at its surface and that it is the local charge distribution, rather than the net charge of the entire proteins, which is the driver for these interactions.[77,78] Positively charged domains on the surface of the corona proteins could therefore mediate the interaction with these ENPs (see below). Also other reports have observed an significant increase in the abundance of human or yeast proteins that bind small, negatively charged ENPs, as silica or silver NPs.[70,79] Eigenheer *et al.*[70] showed that experimental conditions can affect the composition of the protein corona and that electrostatic interactions between the proteins and silver NPs seem to be determinant in the formation of the protein corona in low buffer concentrations, like those used in the present study.

Although electrostatic interactions are likely important, non-electrostatic forces may also influence the protein adsorption.[10,79] In our experimental conditions, the complete removal of the corona proteins from the CdS QD surface required heat-denaturation in the presence of a detergent, as SDS (Fig. 5A). Therefore, whereas electrostatic interactions are required in the first instance, hydrophobic interactions can indeed be involved in the molecular recognition effects which shape and stabilize the corona.[80,81]

Inspection of the amino acid composition revealed a lower frequency of the aromatic residues tyrosine and phenylalanine, and an enrichment of the non-polar residues alanine, glycine and valine in the corona protein sequences as compared with the average amino acid percentages of the yeast proteome (Table S3†). These hydrophobic residues were typically located on the protein outer surface, within structures avoid of secondary regions, as loops or coils, thereby providing the polypeptide chain with a localized high level of flexibility and hence favouring its interaction with the CdS QDs.

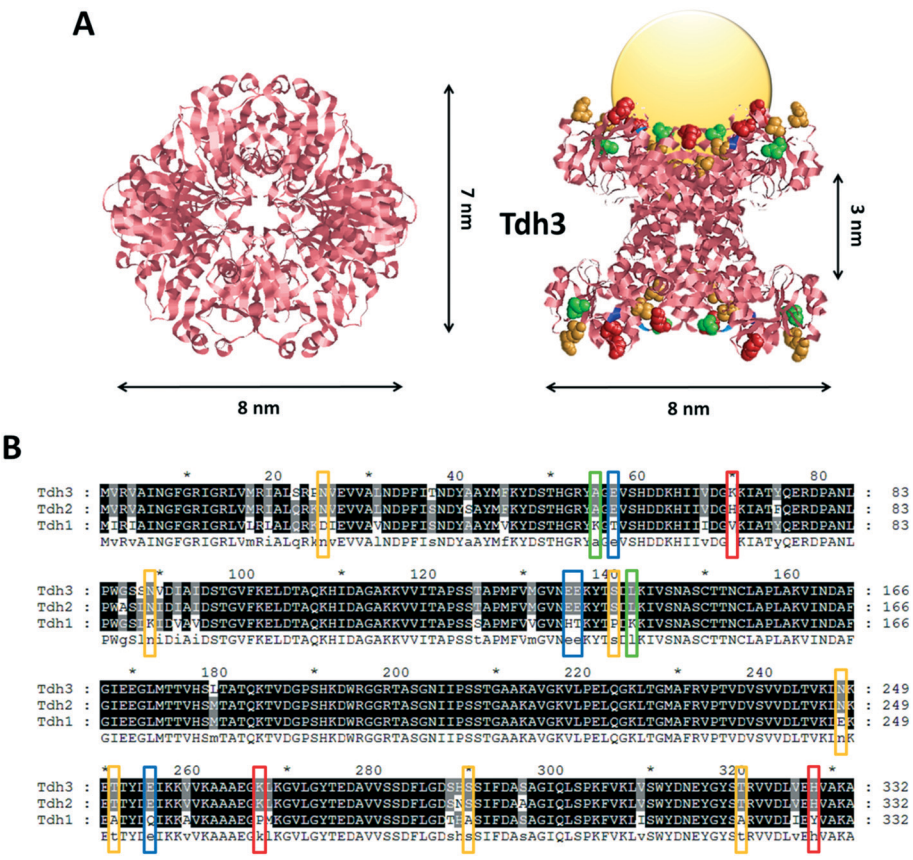

Fig. 6 Putative sites for the binding of Tdh3 to the CdS QD surface. (A) Top and lateral view of the Tdh3 structure (Table S4†). Residues shared between Tdh2 and Tdh3, but absent from Tdh1, are shown in green where hydrophobic, in red where acidic, in orange where polar and in blue where basic. (B) Polypeptide sequence alignment of yeast GAPDH isoforms. The residues shared by Tdh2 and Tdh3, but absent from Tdh1, are boxed. Sequences are aligned with ClustalW Software (http://www.genome.jp/toolsbin/clustalw) and the alignment is plotted using GeneDoc software (http://www.nrbsc.org/old/gfx/genedoc/).

Atomic force microscopy (AFM) analysis of the yeast protein corona showed a lot of small round structures in the absence of aggregates or large clusters of QDs (Fig. S4†). These structures were *ca.* 5 nm in height. As the yeast proteins identified in the hard corona of CdS QDs (Table 1) presented a hydrodynamic diameter of about 3–7 nm, it is possible to hypothesize a competitive adsorption of these proteins on the surface of CdS QDs. An *in silico* analysis of the available crystal structures (Table S4†), based on RasMol, CASTp and PDPsum softwares suggested that the corona proteins folded into either ring (Fig. 5B and C and 6A) or semi-ring-shaped (Fig. 5D) structures. These protein structures characterized by a ring cavity of 5–7 nm diameter (Fig. 5B–D and 6), could clamp ENPs as shown in the QD-binding to the cylindrical cavity of bacterial chaperonin proteins, that enfold these ENPs, giving them high thermal and chemical stability in aqueous media.[73] Interestingly, the self-assembly of peroxiredoxin in a ring-shaped structure having a cavity diameter of 6 nm was recently used to bind gold ENPs;[82] here also, basic residues (especially histidine) were shown to mediate peroxiredoxin interaction with the ENPs.

In this context, it was relevant the study of the ring-shaped structure of Tdh3 (Fig. 6A), the only yeast GAPDH isoform of which the structure is available in the PDB database (Table S4†). Tdh3 shares 96% sequence identity with Tdh2 and only 88% sequence identity with Tdh1 (Fig. 6B). However, while both Tdh2 and Tdh3 were represented in the corona proteins, Tdh1 was not, presumably because it lacks critical residue(s) required for the CdS QD binding. Tdh2 and Tdh3 share several polar (asparagine, threonine and serine) and positively charged (lysine and histidine) residues, which are sited in a pre-formed pocket on the protein surface (Fig. 6); these conserved residues may therefore represent the recognition motifs for Tdh2/3 binding to CdS QDs.

Conclusions

Although recent studies have identified a plethora of proteins in different model systems and explored their role in the formation of the protein corona (see ref. 5, 14, 38, 83 and 84 for some relevant examples), little is known about their role in assessing the safety of an ENP once it is released into the environment. In this study, we address this issue using CdS QDs, whose toxicity is substantially different from that of Cd metal ions in different model systems,[26,85,86] testing their effects in a simple, but "complete" organism, the yeast *S. cerevisiae*. The focus was to isolate the major hard corona proteins to evaluate whether intracellular protein adsorption can explain, at least in part, the negative effects associated to CdS QD treatment *in vivo*.

In yeast, several proteins able to form ring-shaped structures, and implicated in crucial metabolic pathways, form the CdS QD hard corona. With a comprehensive genetic approach we have related the presence of these components on the biocorona with some of the observed molecular and phenotypic effects induced by CdS QD treatment. Our results showed that "free" amounts of some hard corona proteins were strongly reduced upon ENP exposure and a transcriptional modulation of the genes encoding for these proteins could represent a compensatory mechanism of response to their physical sequestration on the ENP surface.

Mutations in some of these genes caused an increased tolerance (not a sensitivity) to CdS QD treatment. This phenotypic effect is consistent with the hypothesis that an aberrant conformation on the CdS QD surface, rather than an inhibition of the function of the hard corona proteins, is responsible for the QD toxicity observed in yeast. ENPs can induce unfolding and a reduced activity of the identified proteins, as observed in the case of GAPDH isoforms,[34] but CdS QD binding to hard corona proteins could mediate non-specific interactions with other cellular components. Misfolded corona proteins can aggregate with itself or other proteins and cause cytotoxicity; in addition, changes in Hsp functionality (*e.g.*, Ssb2 or Hsc82) induced by ENP–protein binding could compromise folding efficiency and target specificity, putting cellular proteostasis at risk.[87]

Therefore, using CdS QDs and yeast cells, we have shown that a reduction of the intracellular levels of the major corona proteins induces a concomitant change on the levels of corresponding mRNAs, in a "risky business" mechanism that can lead to cell death. These data show that the simple identification of adsorbed proteins, without a study of the *in vivo* physiological and molecular responses, is not sufficient to give a real picture of their role on the bioactivity of ENPs.

Future studies will concentrate on the purification of some of the major corona proteins, such as Tdh3, and on the characterization of the specific interaction with CdS QDs. In this way, critical protein epitopes will be identified thus leading to a better understanding of protein corona formation.

Conflicts of interest

The authors declare no competing financial interest.

Acknowledgements

We acknowledge the help of Andrea Faccini (Interdepartmental Measurement Center "Giuseppe Casnati", University of Parma) with the LC-MS/MS and AFM analysis, Gianfranco Galli (Department of Mathematical, Physical and Computer Sciences, University of Parma) with the Z-potential and DLS analysis, and Davide Imperiale with the AAS analysis. We thank Giuliana Germinario for technical help in an early phase of this work. This research was supported by a "Fondi Locali per la Ricerca" grant given in 2014 to R. R., the Interreg Central Europe grant AWAIR (CE1226) and the FACCE-JPI programme (SFS-05-2015: Strategies for crop productivity, stability and quality, project INTENSE).

References

1 A. Nel, T. Xia, L. Madler and N. Li, Toxic potential of materials at the nanolevel, *Science*, 2006, **311**, 622–627.

2 M. Eleftheriadou, G. Pyrgiotakis and P. Demokritou, Nanotechnology to the rescue: using nano-enabled approaches in microbiological food safety and quality, *Curr. Opin. Biotechnol.*, 2017, **44**, 87–93.

3 S. Bakand and A. Hayes, Toxicological Considerations, Toxicity Assessment, and Risk Management of Inhaled Nanoparticles, *Int. J. Mol. Sci.*, 2016, **17**.

4 P. A. Holden, J. L. Gardea-Torresdey, F. Klaessig, R. F. Turco, M. Mortimer and K. Hund-Rinke, *et al.*, Considerations of Environmentally Relevant Test Conditions for Improved Evaluation of Ecological Hazards of Engineered Nanomaterials, *Environ. Sci. Technol.*, 2016, **50**, 6124–6145.

5 I. Lynch, A. Salvati and K. A. Dawson, Protein-nanoparticle interactions: What does the cell see?, *Nat. Nanotechnol.*, 2009, **4**, 546–547.

6 A. E. Nel, L. Madler, D. Velegol, T. Xia, E. M. Hoek and P. Somasundaran, *et al.*, Understanding biophysicochemical interactions at the nano-bio interface, *Nat. Mater.*, 2009, **8**, 543–557.

7 T. Cedervall, I. Lynch, S. Lindman, T. Berggard, E. Thulin and H. Nilsson, *et al.*, Understanding the nanoparticle-protein corona using methods to quantify exchange rates and affinities of proteins for nanoparticles, *Proc. Natl. Acad. Sci. U. S. A.*, 2007, **104**, 2050–2055.

8 D. Walczyk, F. B. Bombelli, M. P. Monopoli, I. Lynch and K. A. Dawson, What the cell "sees" in bionanoscience, *J. Am. Chem. Soc.*, 2010, **132**, 5761–5768.

9 M. P. Monopoli, D. Walczyk, A. Campbell, G. Elia, I. Lynch and F. B. Bombelli, *et al.*, Physical-chemical aspects of protein corona: relevance to in vitro and in vivo biological impacts of nanoparticles, *J. Am. Chem. Soc.*, 2011, **133**, 2525–2534.

10 M. Lundqvist, J. Stigler, G. Elia, I. Lynch, T. Cedervall and K. A. Dawson, Nanoparticle size and surface properties determine the protein corona with possible implications for biological impacts, *Proc. Natl. Acad. Sci. U. S. A.*, 2008, **105**, 14265–14270.

11 A. A. Shemetov, I. Nabiev and A. Sukhanova, Molecular interaction of proteins and peptides with nanoparticles, *ACS Nano*, 2012, **6**, 4585–4602.

12 M. Hadjidemetriou, Z. Al-Ahmady, M. Mazza, R. F. Collins, K. Dawson and K. Kostarelos, In Vivo Biomolecule Corona around Blood-Circulating, Clinically Used and Antibody-Targeted Lipid Bilayer Nanoscale Vesicles, *ACS Nano*, 2015, **9**, 8142–8156.

13 N. Bertrand, P. Grenier, M. Mahmoudi, E. M. Lima, E. A. Appel and F. Dormont, *et al.*, Mechanistic understanding of in vivo protein corona formation on polymeric nanoparticles and impact on pharmacokinetics, *Nat. Commun.*, 2017, **8**, 777.

14 S. Lin, M. Mortimer, R. Chen, A. Kakinen, J. E. Riviere and T. P. Davis, *et al.*, NanoEHS beyond Toxicity – Focusing on Biocorona, *Environ. Sci.: Nano*, 2017, **7**, 1433–1454.

15 T. Miclăuş, V. E. Bochenkov, R. Ogaki, K. A. Howard and D. S. Sutherland, Spatial mapping and quantification of soft and hard protein coronas at silver nanocubes, *Nano Lett.*, 2014, **14**, 2086–2093.

16 D. Docter, D. Westmeier, M. Markiewicz, S. Stolte, S. K. Knauer and R. H. Stauber, The nanoparticle biomolecule corona: lessons learned – challenge accepted?, *Chem. Soc. Rev.*, 2015, **44**, 6094–6121.

17 S. Milani, F. B. Bombelli, A. S. Pitek, K. A. Dawson and J. Radler, Reversible versus irreversible binding of transferrin to polystyrene nanoparticles: soft and hard corona, *ACS Nano*, 2012, **6**, 2532–2541.

18 W. C. Chan and S. Nie, Quantum dot bioconjugates for ultrasensitive nonisotopic detection, *Science*, 1998, **281**, 2016–2018.

19 V. I. Klimov, A. A. Mikhailovsky, S. Xu, A. Malko, J. A. Hollingsworth and C. A. Leatherdale, *et al.*, Optical gain and stimulated emission in nanocrystal quantum dots, *Science*, 2000, **290**, 314–317.

20 F. M. Winnik and D. Maysinger, Quantum dot cytotoxicity and ways to reduce it, *Acc. Chem. Res.*, 2013, **46**, 672–680.

21 I. Concina and A. Vomiero, Metal oxide semiconductors for dye- and quantum-dot-sensitized solar cells, *Small*, 2015, **11**, 1744–1774.

22 E. Oh, R. Liu, A. Nel, K. B. Gemill, M. Bilal and Y. Cohen, *et al.*, Meta-analysis of cellular toxicity for cadmium-containing quantum dots, *Nat. Nanotechnol.*, 2016, **11**, 479–486.

23 M. Sun, Q. Yu, M. Liu, X. Chen, Z. Liu and H. Zhou, *et al.*, A novel toxicity mechanism of CdSe nanoparticles to Saccharomyces cerevisiae: enhancement of vacuolar membrane permeabilization (VMP), *Chem.-Biol. Interact.*, 2014, **220**, 208–213.

24 J. Fan, M. Shao, L. Lai, Y. Liu and Z. Xie, Inhibition of autophagy contributes to the toxicity of cadmium telluride quantum dots in Saccharomyces cerevisiae, *Int. J. Nanomed.*, 2016, **11**, 3371–3383.

25 M. Marmiroli, L. Pagano, F. Pasquali, A. Zappettini, V. Tosato and C. V. Bruschi, *et al.*, A genome-wide nanotoxicology screen of Saccharomyces cerevisiae mutants reveals the basis for cadmium sulphide quantum dot tolerance and sensitivity, *Nanotoxicology*, 2016, **10**, 84–93.

26 F. Pasquali, C. Agrimonti, L. Pagano, A. Zappettini, M. Villani and M. Marmiroli, *et al.*, Nucleo-mitochondrial interaction of yeast in response to cadmium sulfide quantum dot exposure, *J. Hazard. Mater.*, 2017, **324**, 744–752.

27 G. Giaever and C. Nislow, The yeast deletion collection: a decade of functional genomics, *Genetics*, 2014, **197**, 451–465.

28 A. B. Parsons, R. L. Brost, H. Ding, Z. Li, C. Zhang and B. Sheikh, *et al.*, Integration of chemical-genetic and genetic interaction data links bioactive compounds to cellular target pathways, *Nat. Biotechnol.*, 2004, **22**, 62–69.

29 C. S. Lee and G. Belfort, Changing activity of ribonuclease A during adsorption: a molecular explanation, *Proc. Natl. Acad. Sci. U. S. A.*, 1989, **86**, 8392–8396.

30 T. Zoungrana, G. H. Findenegg and W. Norde, Structure, Stability, and Activity of Adsorbed Enzymes, *J. Colloid Interface Sci.*, 1997, **190**, 437–448.

31 L. Shang, Y. Wang, J. Jiang and S. Dong, pH-dependent protein conformational changes in albumin:gold nanoparticle

bioconjugates: a spectroscopic study, *Langmuir*, 2007, **23**, 2714–2721.
32 X. C. Shen, X. Y. Liou, L. P. Ye, H. Liang and Z. Y. Wang, Spectroscopic studies on the interaction between human hemoglobin and CdS quantum dots, *J. Colloid Interface Sci.*, 2007, **311**, 400–406.
33 S. I. Yoo, M. Yang, J. R. Brender, V. Subramanian, K. Sun and N. E. Joo, *et al.*, Inhibition of amyloid peptide fibrillation by inorganic nanoparticles: functional similarities with proteins, *Angew. Chem., Int. Ed.*, 2011, **50**, 5110–5115.
34 S. Ghosh, M. Ray, M. R. Das, A. Chakrabarti, A. H. Khan and D. D. Sarma, *et al.*, Modulation of glyceraldehyde-3-phosphate dehydrogenase activity by surface functionalized quantum dots, *Phys. Chem. Chem. Phys.*, 2014, **16**, 5276–5283.
35 J. H. Shannahan, R. Podila, A. A. Aldossari, H. Emerson, B. A. Powell and P. C. Ke, *et al.*, Formation of a protein corona on silver nanoparticles mediates cellular toxicity via scavenger receptors, *Toxicol. Sci.*, 2015, **143**, 136–146.
36 M. Villani, D. Calestani, L. Lazzarini, L. Zanotti, R. Mosca and A. Zappettini, Extended functionality of ZnO nanotetrapods by solution-based coupling with CdS nanoparticles, *J. Mater. Chem.*, 2012, **22**, 5694.
37 M. Marmiroli, L. Pagano, M. L. Savo Sardaro, M. Villani and N. Marmiroli, Genome-wide approach in Arabidopsis thaliana to assess the toxicity of cadmium sulfide quantum dots, *Environ. Sci. Technol.*, 2014, **48**, 5902–5909.
38 J. Sund, H. Alenius, M. Vippola, K. Savolainen and A. Puustinen, Proteomic characterization of engineered nanomaterial-protein interactions in relation to surface reactivity, *ACS Nano*, 2011, **5**, 4300–4309.
39 M. Bencivenni, A. Faccini, R. Zecchi, F. Boscaro, G. Moneti and A. Dossena, *et al.*, Electrospray MS and MALDI imaging show that non-specific lipid-transfer proteins (LTPs) in tomato are present as several isoforms and are concentrated in seeds, *J. Mass Spectrom.*, 2014, **49**, 1264–1271.
40 K. J. Livak and T. D. Schmittgen, Analysis of relative gene expression data using real-time quantitative PCR and the 2(-Delta Delta C(T)) Method, *Methods*, 2001, **25**, 402–408.
41 R. Ruotolo, F. Tosi, S. Vernarecci, P. Ballario, A. Mai and P. Filetici, *et al.*, Chemogenomic profiling of the cellular effects associated with histone H3 acetylation impairment by a quinoline-derived compound, *Genomics*, 2010, **96**, 272–280.
42 T. A. Binkowski, S. Naghibzadeh and J. Liang, CASTp: Computed Atlas of Surface Topography of proteins, *Nucleic Acids Res.*, 2003, **31**, 3352–3355.
43 E. Boles, F. Schulte, T. Miosga, K. Freidel, E. Schluter and F. K. Zimmermann, *et al.*, Characterization of a glucose-repressed pyruvate kinase (Pyk2p) in Saccharomyces cerevisiae that is catalytically insensitive to fructose-1,6-bisphosphate, *J. Bacteriol.*, 1997, **179**, 2987–2993.
44 A. K. Pearce, K. Crimmins, E. Groussac, M. J. Hewlins, J. R. Dickinson and J. Francois, *et al.*, Pyruvate kinase (Pyk1) levels influence both the rate and direction of carbon flux in yeast under fermentative conditions, *Microbiology*, 2001, **147**, 391–401.
45 J. T. Pronk, H. Yde Steensma and J. P. Van Dijken, Pyruvate metabolism in Saccharomyces cerevisiae, *Yeast*, 1996, **12**, 1607–1633.
46 J. R. Dickinson, L. E. Salgado and M. J. Hewlins, The catabolism of amino acids to long chain and complex alcohols in Saccharomyces cerevisiae, *J. Biol. Chem.*, 2003, **278**, 8028–8034.
47 M. A. Sirover, New nuclear functions of the glycolytic protein, glyceraldehyde-3-phosphate dehydrogenase, in mammalian cells, *J. Cell. Biochem.*, 2005, **95**, 45–52.
48 A. E. Ringel, R. Ryznar, H. Picariello, K. L. Huang, A. G. Lazarus and S. G. Holmes, Yeast Tdh3 (glyceraldehyde 3-phosphate dehydrogenase) is a Sir2-interacting factor that regulates transcriptional silencing and rDNA recombination, *PLoS Genet.*, 2013, **9**, e1003871.
49 M. G. Sandbaken and M. R. Culbertson, Mutations in elongation factor EF-1 alpha affect the frequency of frameshifting and amino acid misincorporation in Saccharomyces cerevisiae, *Genetics*, 1988, **120**, 923–934.
50 S. M. Chuang, L. Chen, D. Lambertson, M. Anand, T. G. Kinzy and K. Madura, Proteasome-mediated degradation of cotranslationally damaged proteins involves translation elongation factor 1A, *Mol. Cell. Biol.*, 2005, **25**, 403–413.
51 C. M. Spahn, M. G. Gomez-Lorenzo, R. A. Grassucci, R. Jorgensen, G. R. Andersen and R. Beckmann, *et al.*, Domain movements of elongation factor eEF2 and the eukaryotic 80S ribosome facilitate tRNA translocation, *EMBO J.*, 2004, **23**, 1008–1019.
52 F. J. Triana-Alonso, K. Chakraburtty and K. H. Nierhaus, The elongation factor 3 unique in higher fungi and essential for protein biosynthesis is an E site factor, *J. Biol. Chem.*, 1995, **270**, 20473–20478.
53 F. Willmund, M. del Alamo, S. Pechmann, T. Chen, V. Albanese and E. B. Dammer, *et al.*, The cotranslational function of ribosome-associated Hsp70 in eukaryotic protein homeostasis, *Cell*, 2013, **152**, 196–209.
54 J. Imai and I. Yahara, Role of HSP90 in salt stress tolerance via stabilization and regulation of calcineurin, *Mol. Cell. Biol.*, 2000, **20**, 9262–9270.
55 E. A. Franzosa, V. Albanese, J. Frydman, Y. Xia and A. J. McClellan, Heterozygous yeast deletion collection screens reveal essential targets of Hsp90, *PLoS One*, 2011, **6**, e28211.
56 S. N. Petrache Voicu, D. Dinu, C. Sima, A. Hermenean, A. Ardelean and E. Codrici, *et al.*, Silica Nanoparticles Induce Oxidative Stress and Autophagy but Not Apoptosis in the MRC-5 Cell Line, *Int. J. Mol. Sci.*, 2015, **16**, 29398–29416.
57 K. Sundarraj, A. Raghunath, L. Panneerselvam and E. Perumal, Iron oxide nanoparticles modulate heat shock proteins and organ specific markers expression in mice male accessory organs, *Toxicol. Appl. Pharmacol.*, 2017, **317**, 12–24.
58 Y. Gong, Y. Kakihara, N. Krogan, J. Greenblatt, A. Emili and Z. Zhang, *et al.*, An atlas of chaperone-protein interactions in Saccharomyces cerevisiae: implications to protein folding pathways in the cell, *Mol. Syst. Biol.*, 2009, **5**, 275.

59 B. Bukau and A. L. Horwich, The Hsp70 and Hsp60 chaperone machines, *Cell*, 1998, **92**, 351–366.

60 S. C. Gupta, A. Sharma, M. Mishra, R. K. Mishra and D. K. Chowdhuri, Heat shock proteins in toxicology: how close and how far?, *Life Sci.*, 2010, **86**, 377–384.

61 G. M. Mortimer, N. J. Butcher, A. W. Musumeci, Z. J. Deng, D. J. Martin and R. F. Minchin, Cryptic epitopes of albumin determine mononuclear phagocyte system clearance of nanomaterials, *ACS Nano*, 2014, **8**, 3357–3366.

62 G. Klein, C. Mathe, M. Biola-Clier, S. Devineau, E. Drouineau and E. Hatem, *et al.*, RNA-binding proteins are a major target of silica nanoparticles in cell extracts, *Nanotoxicology*, 2016, **10**, 1555–1564.

63 R. Ruotolo, G. Marchini and S. Ottonello, Membrane transporters and protein traffic networks differentially affecting metal tolerance: a genomic phenotyping study in yeast, *Genome Biol.*, 2008, **9**, R67.

64 I. Lynch, K. A. Dawson and S. Linse, Detecting cryptic epitopes created by nanoparticles, *Sci. STKE*, 2006, **2006**, pe14.

65 Z. J. Deng, M. Liang, M. Monteiro, I. Toth and R. F. Minchin, Nanoparticle-induced unfolding of fibrinogen promotes Mac-1 receptor activation and inflammation, *Nat. Nanotechnol.*, 2011, **6**, 39–44.

66 F. Chiti and C. M. Dobson, Protein misfolding, functional amyloid, and human disease, *Annu. Rev. Biochem.*, 2006, **75**, 333–366.

67 R. E. Smith and R. MacQuarrie, The role of cysteine residues in the catalytic activity of glycerol-3-phosphate dehydrogenase, *Biochim. Biophys. Acta*, 1979, **567**, 269–277.

68 L. McAlister and M. J. Holland, Differential expression of the three yeast glyceraldehyde-3-phosphate dehydrogenase genes, *J. Biol. Chem.*, 1985, **260**, 15019–15027.

69 A. Linck, X. K. Vu, C. Essl, C. Hiesl, E. Boles and M. Oreb, On the role of GAPDH isoenzymes during pentose fermentation in engineered Saccharomyces cerevisiae, *FEMS Yeast Res.*, 2014, **14**, 389–398.

70 R. Eigenheer, E. R. Castellanos, M. Y. Nakamoto, K. T. Gerner, A. M. Lampeb and K. E. Wheeler, Silver nanoparticle protein corona composition compared across engineered particle properties and environmentally relevant reaction conditions, *Environ. Sci.: Nano*, 2014, **2014**, 238–247.

71 C. D. Walkey, J. B. Olsen, F. Song, R. Liu, H. Guo and D. W. Olsen, *et al.*, Protein corona fingerprinting predicts the cellular interaction of gold and silver nanoparticles, *ACS Nano*, 2014, **8**, 2439–2455.

72 A. Wang, Y. R. Perera, M. B. Davidson and N. C. Fitzkee, Electrostatic Interactions and Protein Competition Reveal a Dynamic Surface in Gold Nanoparticle-Protein Adsorption, *J. Phys. Chem. C. Nanomater. Interfaces*, 2016, **120**, 24231–24239.

73 D. Ishii, K. Kinbara, Y. Ishida, N. Ishii, M. Okochi and M. Yohda, *et al.*, Chaperonin-mediated stabilization and ATP-triggered release of semiconductor nanoparticles, *Nature*, 2003, **423**, 628–632.

74 Q. Wang, Y. Kuo, Y. Wang, G. Shin, C. Ruengruglikit and Q. Huang, Luminescent properties of water-soluble denatured bovine serum albumin-coated CdTe quantum dots, *J. Phys. Chem. B*, 2006, **110**, 16860–16866.

75 V. Poderys, M. Matulionyte, A. Selskis and R. Rotomskis, Interaction of Water-Soluble CdTe Quantum Dots with Bovine Serum Albumin, *Nanoscale Res. Lett.*, 2011, **6**, 9.

76 A. Kale, Y. Bao, Z. Zhou, P. E. Prevelige and A. Gupta, Directed self-assembly of CdS quantum dots on bacteriophage P22 coat protein templates, *Nanotechnology*, 2013, **24**, 045603.

77 F. E. Regnier, The role of protein structure in chromatographic behavior, *Science*, 1987, **238**, 319–323.

78 J. Meissner, A. Prause, B. Bharti and G. H. Findenegg, Characterization of protein adsorption onto silica nanoparticles: influence of pH and ionic strength, *Colloid Polym. Sci.*, 2015, **293**, 3381–3391.

79 S. Tenzer, D. Docter, S. Rosfa, A. Wlodarski, J. Kuharev and A. Rekik, *et al.*, Nanoparticle size is a critical physicochemical determinant of the human blood plasma corona: a comprehensive quantitative proteomic analysis, *ACS Nano*, 2011, **5**, 7155–7167.

80 V. Uskokovic, Z. Castiglione, P. Cubas, L. Zhu, W. Li and S. Habelitz, Zeta-potential and particle size analysis of human amelogenins, *J. Dent. Res.*, 2010, **89**, 149–153.

81 N. Duran, C. P. Silveira, M. Duran and D. S. Martinez, Silver nanoparticle protein corona and toxicity: a mini-review, *J. Nanobiotechnol.*, 2015, **13**, 55.

82 M. Ardini, F. Giansanti, L. Di Leandro, G. Pitari, A. Cimini and L. Ottaviano, *et al.*, Metal-induced self-assembly of peroxiredoxin as a tool for sorting ultrasmall gold nanoparticles into one-dimensional clusters, *Nanoscale*, 2014, **6**, 8052–8061.

83 T. A. Faunce, J. White and K. I. Matthaei, Integrated research into the nanoparticle-protein corona: a new focus for safe, sustainable and equitable development of nanomedicines, *Nanomedicine*, 2008, **3**, 859–866.

84 F. Pederzoli, G. Tosi, M. A. Vandelli, D. Belletti, F. Forni and B. Ruozi, Protein corona and nanoparticles: how can we investigate on?, *Wiley Interdiscip. Rev.: Nanomed. Nanobiotechnol.*, 2017, **9**.

85 M. Marmiroli, D. Imperiale, L. Pagano, M. Villani, A. Zappettini and N. Marmiroli, The Proteomic Response of Arabidopsis thaliana to Cadmium Sulfide Quantum Dots, and Its Correlation with the Transcriptomic Response, *Front. Plant Sci.*, 2015, **6**, 1104.

86 L. Paesano, A. Perotti, A. Buschini, C. Carubbi, M. Marmiroli and E. Maestri, *et al.*, Markers for toxicity to HepG2 exposed to cadmium sulphide quantum dots; damage to mitochondria, *Toxicology*, 2016, **374**, 18–28.

87 M. Brehme and C. Voisine, Model systems of protein-misfolding diseases reveal chaperone modifiers of proteotoxicity, *Dis. Models & Mech.*, 2016, **9**, 823–838.